Final OMLC Progress Report

for

Phase II of AF063-003 under Air Force Contract FA9550-09-C-0051

Scott Prahl
Oregon Medical Laser Center
Providence St. Vincent Medical Center
9205 SW Barnes Rd
Portland, Oregon 97225

Kirk Price
nLIGHT Corporation
5408 NE 88th St, Bldg. E
Vancouver, WA 98665

Report Documentation Page

Form Approved
OMB No. 0704-0188

1. REPORT DATE	2. REPORT TYPE	3. DATES COVERED
24 FEB 2011		**00-11-2008 to 00-02-2011**

4. TITLE AND SUBTITLE	5a. CONTRACT NUMBER
Photochemical Tissue Bonding For Military Medical Applications Practical Low Cost Low Damage Blood Vessel Repair: Albumin Stent Bonded With 19xx nm Laser	5b. GRANT NUMBER
	5c. PROGRAM ELEMENT NUMBER
6. AUTHOR(S)	5d. PROJECT NUMBER
	5e. TASK NUMBER
	5f. WORK UNIT NUMBER
7. PERFORMING ORGANIZATION NAME(S) AND ADDRESS(ES) **Oregon Medical Laser Center,9205 SW Barnes Rd,,Portland,OR,97225**	8. PERFORMING ORGANIZATION REPORT NUMBER **; AFRL-OSR-VA-TR-11-040**
9. SPONSORING/MONITORING AGENCY NAME(S) AND ADDRESS(ES)	10. SPONSOR/MONITOR'S ACRONYM(S)
	11. SPONSOR/MONITOR'S REPORT NUMBER(S) **AFRL-OSR-VA-TR-11-040**

12. DISTRIBUTION/AVAILABILITY STATEMENT
Approved for public release; distribution unlimited

13. SUPPLEMENTARY NOTES

14. ABSTRACT

nLIGHT and Oregon Medical Laser Center have developed a low cost, highly effective method to repair blood vessels damaged by trauma or surgery. OMLC has developed an method for extruding albumin stents, inserting these albumin stents for blood vessel reinforcement, and using a 19xx nm laser diode to effectively weld the blood vessel. We have performed tensile tests, burst tests, and are preparing for final live animal studies to test the effectiveness of this blood vessel repair system.

15. SUBJECT TERMS

16. SECURITY CLASSIFICATION OF:			17. LIMITATION OF ABSTRACT	18. NUMBER OF PAGES	19a. NAME OF RESPONSIBLE PERSON
a. REPORT	b. ABSTRACT	c. THIS PAGE			
unclassified	**unclassified**	**unclassified**	**Same as Report (SAR)**	**30**	

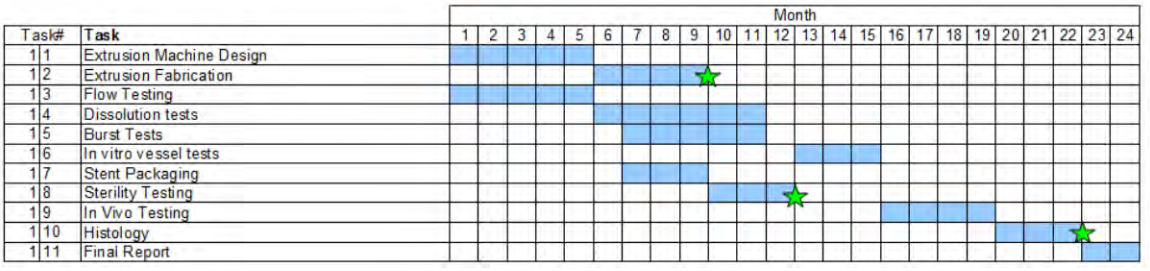

Overview

Our original timeline is shown above. All tasks except the animal trial have been completed. We are awaiting IACUC approval before commencing the animal trial.

Quarter 1

We began initial extrusion device prototyping and design.

Quarter 2

we fabricated our proposed extrusion design. This design incorporated a screw plunger and temperature control that allowed a standard syringe to be inserted. The screw provided the force needed to press the viscous albumin through the extrusion device. The temperature control allows the albumin to be maintained at 50°C to reduce its viscosity.

Quarter 3

We started in vitro testing. We used our temperature-controlled extruder to create albumin stents with an outside diameter ranging from 2–5 mm. The critical detail needed for stent production was that the extruder must be controlled at 49±1°C and the concentration of the albumin in the syringe should be 56.0±0.5% weight/volume. At lower temperatures, the albumin was too viscous to be extruded. At higher temperatures, the albumin coagulated. At lower concentrations, the albumin was too fluid and would not retain its shape. At higher concentrations, the albumin would not flow through the extruder.

Quarter 4

We used our temperature-controlled extruder to create albumin stents with an outside diameter from 2 mm and various inner lumen diameters. Dissolution studies in flowing blood indicated that the stents

resorbed in a few minutes. This was important because if the stents dissolved to quickly (seconds) then they would not remain solid while being laser welded in place by the surgeon. On the other hand, if the stents took hours or days to resorb, then the anastomosis site could be the nidus for clotting or stenosis.

Quarter 5

We completely redesigned our extrusion device because the plastic syringe was deforming during extrusion. The new device was fabricated a new device completely out of aluminum. This allowed us to reach much greater pressures during the extrusion process and we have a much more robust reliable extruder.

Quarter 6

We developed standard dissolution measurements. Determined that blood and saline dissolve stents at the same rate. Determined that gamma sterilization procedure does not affect dissolution. Determined that flow rate affects the dissolution rate, but that the dissolution scales with the total flow.

Quarter 7

We completed all in vitro laser anastomosis testing. Produced sterile albumin and stents for in vivo animal trial.

Quarter 8

We completed IACUC paperwork and started submission process. Prepared paper describing our work for *Lasers in Surgery and Medicine*.

Objectives

Task 1.1, Extrusion machine design

One critical element of the design of the albumin stent extruder was that it had to be sterilizable and compatible with standard medical grade syringes. Another consideration was that the extrusion device would not waste large amounts of albumin and therefore needed to be small, efficient, and easily cleaned.

The extruder used a single-screw, sterilizable albumin stent extrusion core (figure 1, bottom right) connected to a 6 ml syringe filled with albumin. To get the albumin to flow through the device the albumin was heated. We developed a temperature-controlled extrusion setup (figure 2, top) to house the extrusion core to produce albumin stents (15 mm length, 1 mm inner diameter, 3 mm outer diameter). Albumin at a concentration threshold between liquid and solid so that

the albumin would flow when heated and solidify upon cooling. The new design included two thermocouples (Omega Engineering, Stamford, CT), four heating rods (Omega Engineering, Stamford, CT), an aluminum holder and a vice. This device allowed us to heat and press albumin from a 6 ml syringe through four 2 mm diameter holes, through an extrusion barrel and into the air. By the time the albumin exited the cavity, the stent shape was set by cooling in the air.

This device was tested with human and porcine albumin with concentrations of 50-65%. A few deformed stents were extruded and some work remained before we would produce stents that would be good enough for the in vivo testing anticipated in year two. We produced extruders with three different outer diameter and needles with three different diameters as well. This allowed us to vary the inner stent diameter as well as the stent wall thickness.


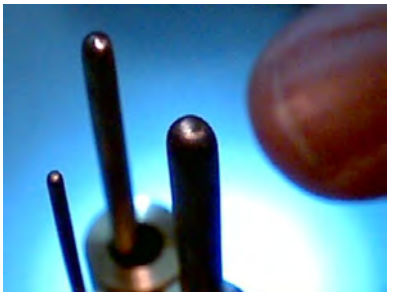
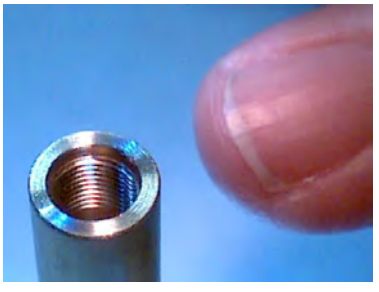


Figure 1: Initial extruder design that used standard cannula needles attached to the lock on the syringe. After a syringe is filled with concentrated albumin (60-64% weight/volume), the albumin is pushed out of the syringe and through the small ports drilled through the tapered section of the needle (top left). The needle itself is sealed shut (top right picture at right showing the tips of three separate needles) at the tip and serves as the inner support when making stents. The threads on the needle in the top right picture are then screwed into the outer conduit (bottom left). The original albumin stent extrusion core attached to a 6 ml syringe filled with albumin and a slightly larger stent extrusion barrel and extrusion center (bottom right).

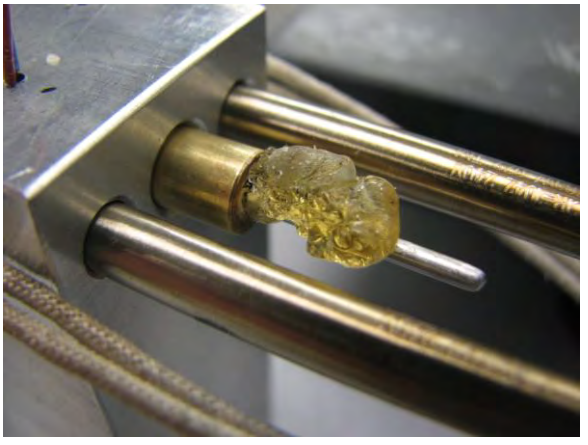

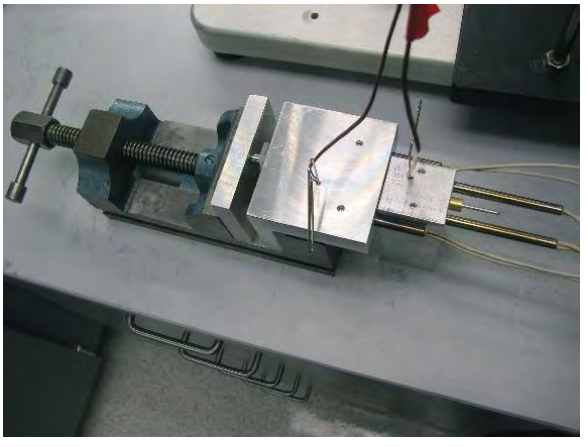

Figure 2: (top) Close-up of the end of the extrusion core with albumin exiting the core and hardening. This is 56.2% albumin. This shows the drawbacks of the first design. First, the extrusion core will not remain concentric with the extrusion tube. Second the albumin is too liquid when it leaves the extrusion tube and fails to retain its shape when leaving. (bottom) The heated extrusion setup. The large square of albumin has the 6 ml syringe of albumin fully inserted. The small square block of aluminum on the far right has the extrusion core barely extending from the block face in the center. The two horizontal rods are the heating cores for thermal control. The vice is used to force the albumin through the syringe and out the extrusion core.

Task 1.1, Extrusion machine redesign

After trying the original design for a number of weeks, it became apparent that reproducible stents could not be manufactured with such a device. The best extruded stents were at the highest albumin concentrations. The pressure necessary to extrude the albumin caused the plastic syringe to deform. We decided to fabricate an all-metal device (figure 3) that allowed us to make stents with outer diameters from 2.0 to 5.0 mm in 0.5 mm increments. The device was fabricated out of aluminum and anodized. Sterility was achieved by autoclaving all parts before use.

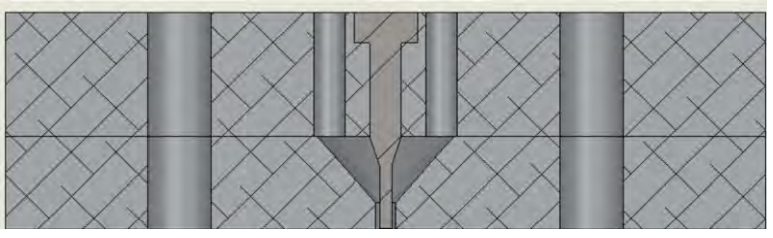

Figure 3: Cross-section of the breaker plate (top) and reducing orifice (bottom). The central dark area is ejector pin that protrudes into the reducing orifice where the albumin is formed into a hollow cylinder. The albumin flows down from the top through the channels adjacent to the central ejector pin and into the reducing orifice. The outer diameter of the stent is determined by the size of the orifice and the inner diameter is determined by the size of the reducing pin.

The new extruder has a cylindrical plunger bolted to the moveable part of a vise (figure 4, lower right). The plunger pushes albumin placed in a through hole in the L-shaped assembly mounted on the left side of the vise past a breaker plate, through a concentrator, and out into the air. We found that no temperature control was necessary to extrude alumin stents as long as the albumin concentrations were between 55.5 and 57.0 % (wt/wt). This simplified the manufacturing process tremendously.

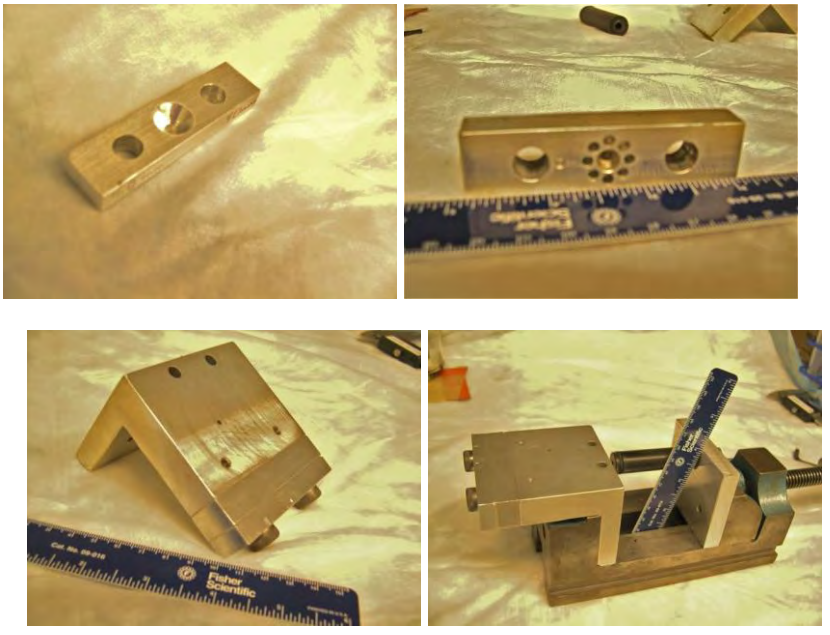

Figure 4: Photographs of the reducing orifice (top left), the breaker plate (top right), the assembled L-shape (bottom left). Complete extruder (bottom right) shows the plunger that is used to drive albumin through the L-shape. The plunger in the center next to the ruler. The concentrator and breaker plate are the last two aluminum pieces on the left.

Task 1.2, Extrusion Fabrication

Figure 5: (left) An albumin tube being extruded. (right) Stents being cut into 17 mm sections with a scalpel.

Human serum albumin (HSA) (Albuminar, CSL Behring, IL) was concentrated to 55.0–57.4% (all albumin concentrations expressed as w/w) by evaporation of water through 25 kDA molecular weight cutoff dialysis tubing (Spectra/Por, Spectrum Laboratories, CA) over 10–16 hours. This concentration method proved advantageous over our previous pressure filtration method which was difficult to monitor, required extended continuous observation, failed to eliminate spatial concentration gradients, and often led to filter rupture.

During dialysis, the albumin concentration C_{HSA} was monitored by weighing the tubing assembly at regular intervals and calculating C_{HSA} based on the weight loss from the starting weight. Once the target concentration was reached, the dialysis tubing was removed and the concentrated albumin was vacuum sealed in a foil pouch. Radial concentration gradients were noted at this point because the outermost surface was much more rigid than the inner albumin. After sealed storage in the foil bags for 96 hours or more, the texture of the albumin was essentially homogenous. To verify these tactile observations, 3 core and 3 surface refractive index measurements were taken from 3 different cross sections of a cylinder of 55.4% HSA immediately after dialysis, then again from adjacent cross sections after 96 hours of sealed storage.

A cylinder of concentrated albumin was inserted into a purpose-built, vise-mounted extruder. A set of dies with circular orifices

ranging from 1.5–5.0 mm in 0.5 mm increments determined the stent outer diameter, while concentric pins (0.7–2.7 mm) controlled the inner diameter. The die and pin with the desired stent dimensions were assembled and mounted on the extruder. A piston forced the concentrated albumin through the die. The extruded tube of albumin was collected on a sheet of rubberized Teflon to prevent curling or drooping and cut into 100 mm lengths with a razor blade. This process continued until all the concentrated albumin was extruded.

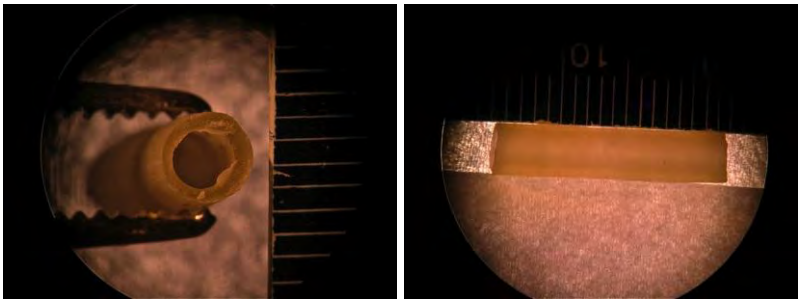

Figure 6: A finished 4 mm outer-diameter stent. The markings on the ruler are in millimeters.

The 100 mm long albumin tubes were allowed to dry for 10–30 minutes at room temperature; at this point the tubes were firm enough to be cut without slumping. The albumin tubes were cut into 17 mm long stents by rolling back and forth gently under a scalpel edge. This cutting technique minimized the tendency of the stent to pinch shut. Finished stents were stored individually in 1.5 mL micro-centrifuge tubes. Each lot of stents was sealed in an aluminum pouch and (except for non-irradiated controls) γ-irradiated at 25–40 kGy (Steris, Isomedix, IL). The stents were stored at room temperature after sterilization.

Finished stents were viewed through a stereomicroscope (MZ-12, Leica, GMBH) to observe surface uniformity. To monitor the accuracy and precision of the dimensions, five stents were randomly selected from five extrusions of 3.0/1.1 to 4/2.7 stents with concentrations ranging from 55.0% to 57.4%. The outer diameter d_{outer} was measured with digital calipers (Absolute Digimatic, Mituyo Corp) and reported as percent change from the orifice diameter: $1-d_{outer}/d_{orifice}$ where $d_{orifice}$ is the diameter of the die orifice.

Measurement of stent outer diameters revealed that the extrudate had a tendency to shrink by 5±3%. Only one of the 25 stents measured had a larger outer diameter than the die orifice, presumably because it encountered mild compression while exiting the die.

Magnified observation revealed that stents made with *CHSA*<55.5 % deformed under light mechanical stress and developed deep cracks when sectioned after drying; the dry stents tended to break into large pieces on light handling. Stents made from slightly higher albumin concentrations (56.5±0.5%) did not deform under light mechanical stress and could still be bent under moderate pressure, especially if warmed slightly (i.e., by a surgeon's hands to accommodate a curved anastomosis site) without causing cracks or lumenal collapse. Concentrations above 57.0% required considerably more force to extrude and these stents did not deform under light mechanical stress. Shallow surface cracks became discernible immediately after exiting the die, and small (~10 μm thick) sheets flecked off. Deep cracks were not observed, nor did stents break into large pieces. Small ~10 μm longitudinal striations were observed at all extrudate concentrations.

Magnified observation of inner lumen surfaces after dividing stents longitudinally revealed inner surfaces with similar properties to outer surfaces. No closure or narrowing of the inner lumen was observed for 55.5–57.4% extrudate concentrations.

Task 1-3 Flow testing

Dissolution coefficients were measured by pumping blood through stents at known flow rates. To approximate intravascular implantation, stents were inserted into a 30 mm long section of tubing with lumen diameter of 3.17 mm for the 3.0 mm outer diameter stents and 4.35 mm for the 4.0 mm outer diameter stents. Fluid was pumped through the stent for 5–20 minutes until the stent was completely dissolved. The fluid was kept at 37°C and recirculated through the tubing for 20 minutes prior to dissolution to ensure uniform temperature throughout the system. It was not recirculated after beginning the dissolution.

In citrated whole porcine blood, dissolution progress was monitored by weighing the stent-containing section of tubing before after ten seconds, and then at 30-second intervals. Flow was stopped before disconnecting the tubing section, which was quickly rinsed with 2 mL of ice water and shaken to remove trapped liquid before weighing. Each stent was used for only one weight measurement, and 3 stents were measured per time point. Seventeen stents were used to measure dissolution progress over 2.5 minutes of flow. The dissolution coefficient, V_{blood}^{diss}, representing the volume required for stent dissolution per unit mass was calculated by taking the ratio of the change in the stent mass to that volume of fluid that passed through the stent.

PBS dissolution coefficients were obtained with the same pump and tubing configuration used to measure dissolution coefficients in blood (after thorough cleaning and cycling with PBS at 37°C for 20 minutes). For each stent, the eluent was collected in cuvettes for UV absorbance measurement after ten seconds, and then at 30 second intervals. Flow was not interrupted during the dissolution. When it became apparent that dissolution depended primarily on the solvent volume passed through the stent, the fraction of the stent remaining $f(V)$ was expressed as a function of volume, as the ratio of 278 nm absorption

$$f(V) = \frac{A278\,nm^{(V)}}{A278\,nmmax} \tag{1}$$

where $A278\,nm^{(V)}$ is the corrected absorbance for the volume V, and $A278\,nmmax$ is the highest absorbance measured in each dissolution. $A278\,nmmax$ occurred at 10 and 30 s in all tests. The dissolution

coefficient (in mL/mg), was reported as the solvent volume $V_{10\%}$ corresponding to $f(V)$=0.1, divided by 90% of the initial mass of the stent m_0:

$$V_{PBS}^{diss} = \frac{V_{10\%}}{0.9 m_0} \tag{2}$$

All tests comparing blood and PBS were performed with a flow rate of 139 mL/min on 3.0/1.6 stents. The solubility of 3.0/1.6 stents was measured at PBS flow rates ranging from 27–139 mL/min. Another series of tests comparing the effect of wall thickness on solubility was performed in PBS on 4.0 mm outer diameter stents with inner diameters of either 1.1 or 2.7 mm at 100 mL/min.

As the flow rate decreased, the time to reach 10% of *Amax* increased from 111 s at 139 mL/min to 495 s at 27 mL/min. Plotting C_{HSA} against volume rather than time suggested that stent dissolution depended primarily on total solvent volume regardless of flow rate (Fig. 7, Table 1). $\frac{A^{(V)}}{A^{max}}$ decreased to a common baseline after approximately 236 mL had passed through the stent. No stent required more than 4.2 mL/mg to reach 10 % of *Amax*.

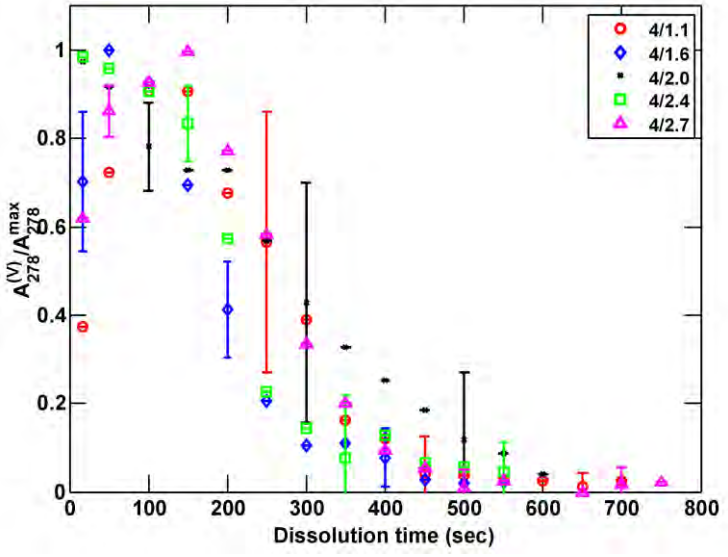

Figure 7: $A_{278\,nm}/A_{278\,nm}^{max}$ vs. volume for 4 mm outer diameter stents with varied inner lumen diameters. Some error bars (representing 1 standard deviation) have been omitted for clarity. No statistically-significant difference (p>0.45) was observed as a function of inner lumen diameter.

Dissolution coefficients ranged from 2.0 to 2.6 mL/mg, with no clear or significant trends arising as a function of wall thickness. The average dissolution volume over all wall thicknesses was 2.2±0.5 mL/mg, with no stent requiring more than 3.2 mL/mg to reach 10% of peak absorbance (Table 1).

Test Condition	(N)	Dissolution Coefficient (mL/mg)
blood	17	2.7±4.3
PBS	5	2.7±0.8
27 mL/min	3	2.7±0.4
50 mL/min	4	2.3±0.4
100 mL/min	5	1.9±0.5
139 mL/min	5	2.7±0.8
0.65 mm wall	4	2.1±0.5
1.45 mm wall	4	2.6±0.6
3/1.6	17	2.3±0.6
4/x	17	2.2±0.5

Table 1: Dissolution coefficient comparison from dynamic dissolution tests examining the effects of solvent, flow rate, and stent geometry. All tests at different flow rates were performed on 3/1.6 stents, while all tests comparing different wall thicknesses were performed on 4/x stents at a flow of 100 mL/min. No significant differences were found between groups

For dissolution times less than 1 minute in blood, it was difficult to remove excess liquid held in the small inner lumen before weighing the tubing section. This was apparent in the large variations in the dissolution times (Fig. 8, Table 1).

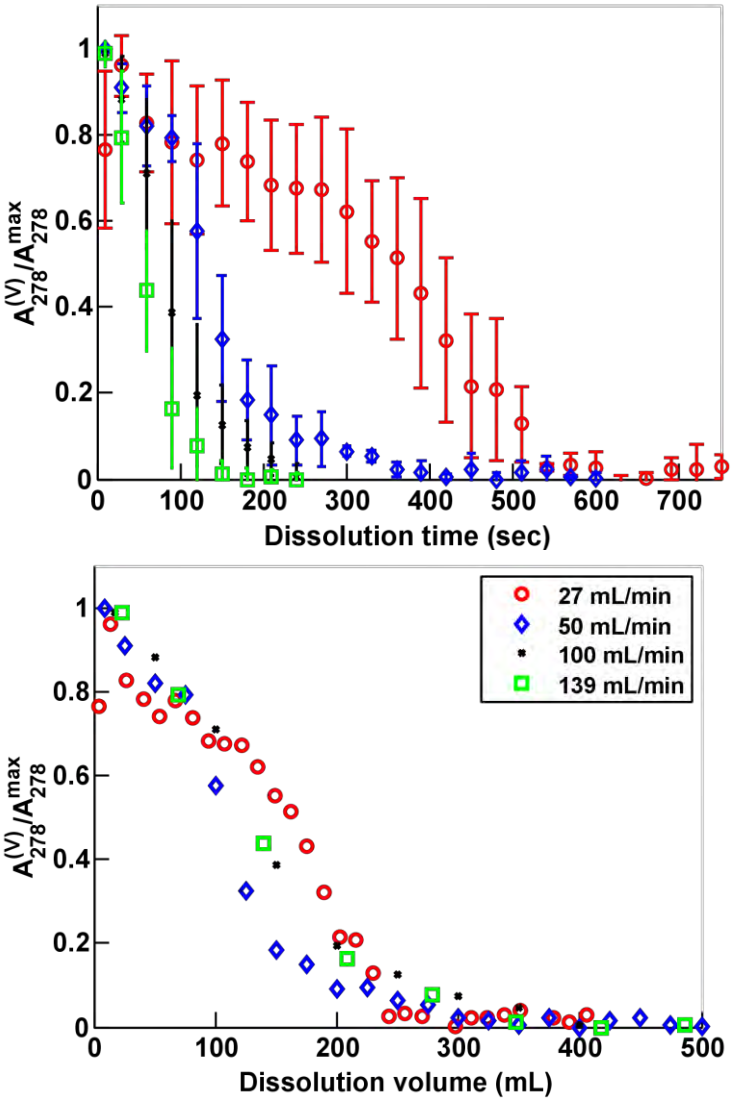

Figure 8: $A_{278}/A^{278}max$ vs. time (top), and $A_{278}/A^{278}max$ vs. volume (bottom) for 3 mm outer diameter stents (with different lumen diameters) in flowing PBS. Error bars represent one standard deviation, and some have been omitted for clarity. Flow rate did not significantly affect normalized dissolution as a function of volume (p>0.15).

The standard deviation was more than five times higher in blood than in PBS. Absorbance measurement was also ~10 times faster.

Task 1-4, Dissolution testing

Static dissolution rates were evaluated by immersing solid albumin cylinders in PBS. The cylinders were extruded using 56% (w/w) HSA with no inner lumen and sectioned to form 12–25 mm long solid cylinders with 2 mm outer diameters. The cylinders were weighed, placed in polyethylene microcentrifuge tubes, divided into 2 equal-numbered groups, and vacuum sealed in foil pouches after purging with nitrogen. One group was γ-irradiated at 25–40 kGy, while the other was stored at room temperature. Each cylinder was dissolved in 5 mL PBS maintained at 37 °C in a disposable glass culture tube (Thermo Fisher Scientific, Inc.). At 100, 200, and 300 s intervals, three irradiated, and three non-irradiated sample tubes were decanted into empty culture tubes. The concentration in each tube was measured spectrophotometrically. The total amount of dissolved albumin was normalized to the initial surface area of the cylinder and reported in $\mu g/mm^2$.

Dissolved albumin concentrations increased from 60 $\mu g/mm^2$ after 100 seconds to 140 $\mu g/mm^2$ after 300 seconds for both irradiated and control stents (Fig. 9). Average dissolution rates were 0.5±0.1 and 0.5±0.2 $\mu g/mm^2/s$, respectively. The dissolution rate is given as the mass of albumin dissolved into solution per second, normalized over the original surface area of the cylinder.

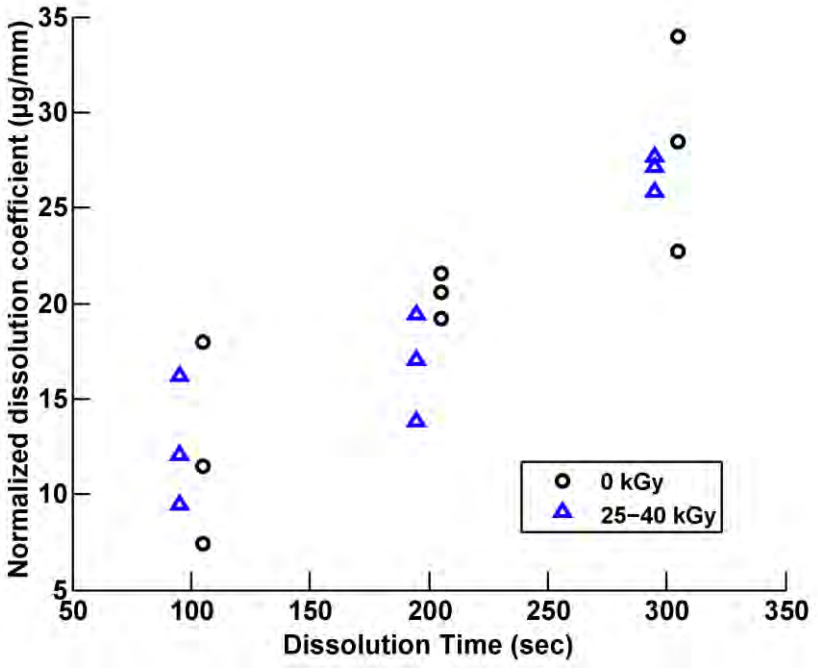

Figure 9: µg HSA dissolved, normalized over surface area vs. time in static dissolution comparing γ-sterilized and control stents in PBS without flow. Irradiated and non-irradiated data points were offset −5 and +5 sec., respectively for clarity. Differences in solubility were not significant at any time point.

Task 1-5, Burst testing

Domestic porcine carotid arteries (Animal Technologies, TX and Sierra Medical Technologies, CA) were harvested into PBS and shipped overnight on ice. All had inner diameters of approximately 4 mm. Vessels were selected at random and sectioned into 3 cm lengths for tensile strength testing, and into 5 cm lengths for burst pressure testing.

Vessels were welded under magnification by a stereoscope (SZ-STB1, Olympus Corp) using albumin solder externally and albumin stents internally to provide internal support. Excess fascia and adventitial tissue were first cut away, and excess moisture was dabbed away with a paper tissue. The vessel was transected with surgical scissors at a right angle. A stent was inserted into the cut end of each vessel, and the ends were drawn into close and uniform contact over the stent. The outer diameter of the stent was chosen to match the vessel inner diameter such that it could be inserted with only slight pressure, but would not slip out under light manipulation during welding.

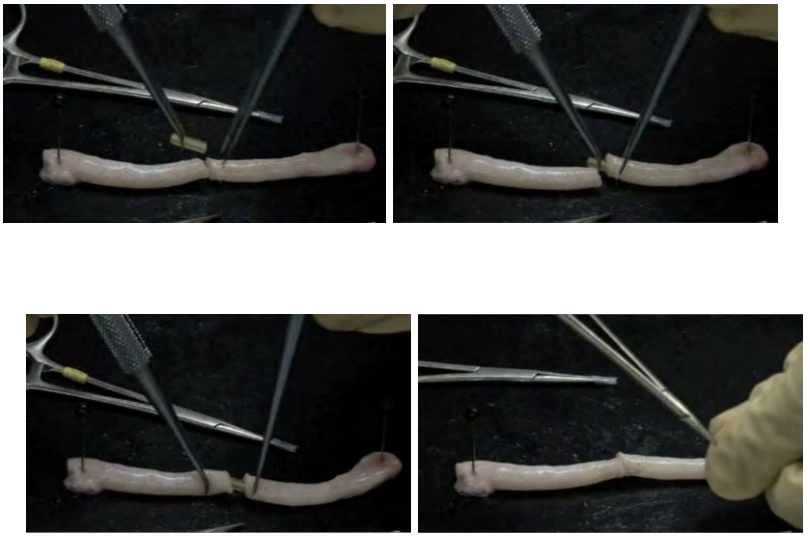

Figure 10: Process of laser anastomosis. Top left shows the two small stent being held by forceps. Top right shows the stent inserted into one vessel. Bottom left shows both stent inside both vessels. Bottom right shows the first of four stay sutures.

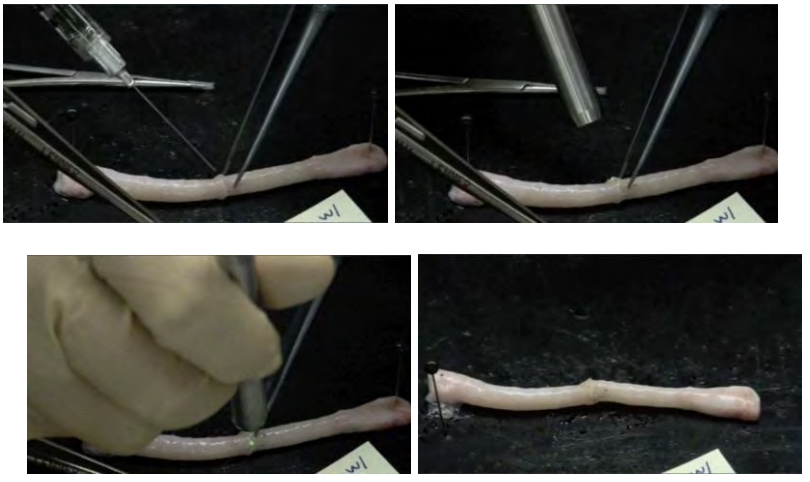

Figure 11: Process of laser anastomosis continued. Top left shows the a syringe dripping 25% albumin onto the outside surface of the vessel. Top right and bottom left shows the laser welding taking place. The completely anastomosed vessel is shown in the bottom right.

Albumin solder was then applied to the anastomosis with a 1.0 mL syringe and a 27 Ga needle. For *CHSA*≤43% (w/w), solder surface tension was low, so minimal manual spreading was necessary to achieve uniform coverage. The solder was denatured with 1.9 micron laser light until a uniform golden-tan color change was observed. A green LED coupled to the laser fiber provided a visible aiming beam. Procedure time was measured as the time from vessel transection to weld completion. Irradiation time was measured as the time the laser was activated, but does not account for small periods of time to reposition the laser spot on the vessel.

Laser spot size was dependent on the focus length, and differed from the aiming beam spot size due to dispersion. A nominal minimum spot size of 0.2 mm at 1.9 microns was measured using laser alignment paper (Zap-It Corp.) with the handpiece 2 mm past the aiming beam focus length. The nominal minimum spot size was used for all anastomoses.

Vessels were immediately placed in sealed polyethylene centrifuge tubes with PBS-moistened paper tissues to prevent dessication and kept at 4°C until mechanical strength testing. Five vessels were welded for each set of weld parameters (except 1 mm wide weld tensile tests, where *N*=7). Welding parameters were independently varied to discern

the optimal parameters. Weld width was varied from 1–3 mm; solder concentration from 22–46% HSA (w/w); laser power from 430–610 mW; and the number of solder layers from 1–3.

Ten vessels were welded with four interrupted 6–0 prolene stay sutures evenly spaced around the anastomosis. To determine if prolonged exposure to moisture degraded the anastomosis, vessels were welded with the most surgically-promising parameters (judged by low weld time, high strength, and reproducibility) and stored submerged in PBS at 4°C for 0 and 5 hours before burst and tensile testing. Five vessels with sutures only, as in conventional surgical application, were burst and tensile tested for comparison.

The output of a pressure transducer (68074-12, Cole-Parmer Inc., IL) precalibrated to produce 25 mV/mmHg was sampled at 15 Hz and digitally recorded (BNC 2120, National Instruments Corp). One-eighth inch barbed tube fittings were inserted into opposite ends of the vessel and were tied down tightly with 1/8" wide umbilical tape. The inlet tube fitting was connected to a peristaltic pump (505Di, Watson-Marlow Inc., MA) drawing from a reservoir of PBS at 23°C. The outlet tube fitting was connected to a T-section with the pressure transducer and a stopcock which could be closed or opened to build or relieve pressure. With the stopcock closed, PBS was pumped into the vessel section until bursting. Burst pressure was reported as the difference between ambient and maximum pressure before bursting.

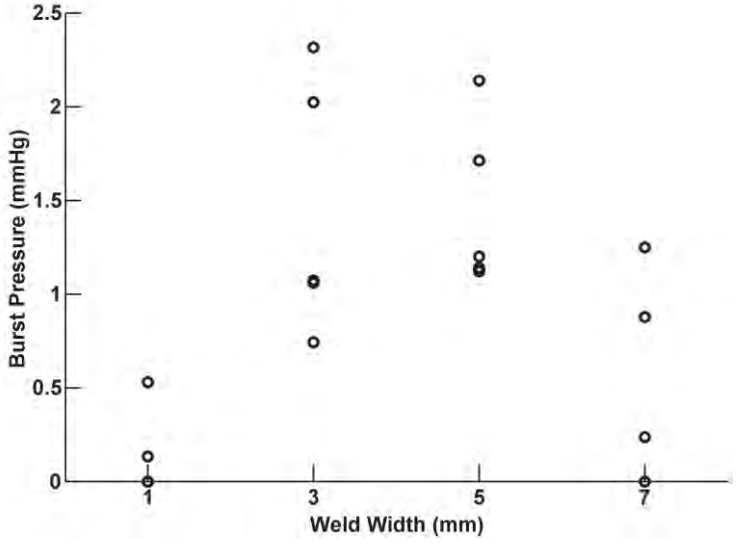

Figure 12: Burst pressure vs. weld width where P=430 mW, n_{layers}=2, C_{solder}=38%. N=5 for all points, except for W=7, where N=4 because a sensor I/O error occurred during testing.

Increasing solder concentration (with P=430 mW, W=3 mm, and n_{layers}=2) led to increases in ultimate tension from 0.5±0.2 N at 22% to 1.3±0.5 N at 43%. At 46%, average tensions decreased slightly to 1.1±0.9 N (Fig. 15). Delamination occurrence and relative standard deviation increased above 38%. All *Csolder*≤38% welds failed by tearing through the denatured albumin sheath, while 20% of 43% welds, and 80% of 46% welds failed by delamination, indicating less consistent adhesion to the vessel than at lower concentrations.

Welds made with laser powers of 430–610 mW (n_{layers}=2, W=3 mm, *Csolder*=38%) had average tensile strengths of 0.8±0.1 to 2.2±0.9 N, with 570 mW yielding the highest strength (Fig. 15). Counter to expectations, increasing laser power did not significantly reduce the irradiation time.

Group	TS (N)	BP (mmHg)
W	2.1±1.0*	231±161
W_{PBS}	0.3±0.2*	–
S	11.6±1.8*	217±92
S,W	4.4±0.7	402±87
S,W_{PBS}	3.3±0.6	458±388

Table 2: Vessels with only continuous sutures (S), only welds (W), and welds with 4 stay sutures (S,W) were tested for tensile strength and burst pressure at the anastomosis. Additional W and W,S were submerged in PBS for hours prior to testing. Asterisks denote statistically-significant difference compared to S,W.

If the anastomosed vessels were submerged in PBS for five hours, maximum tension for *Csolder*=38%, P=570 mW, W=3 mm, *nlayers*=2 sutureless welds decreased from 2.1±0.9 N to 0.3±0.2 N, indicating that

vessels welded without stay sutures would not retain adequate tensile strength *in vivo*. With the addition of 4 stay sutures, average maximum tension still decreased from 4.4±0.8 N to 3.3±0.6 N after storage (Fig. 13 top, Table 2). Burst pressure averages in welded, stay-sutured vessels did not decrease significantly (p=0.8) after storage in PBS, but the standard deviation increased from 86 to 388 mm Hg (Fig. 13 top). Although the denatured albumin cuff at the anastomosis did not dissolve in PBS, it swelled visibly and became more friable.

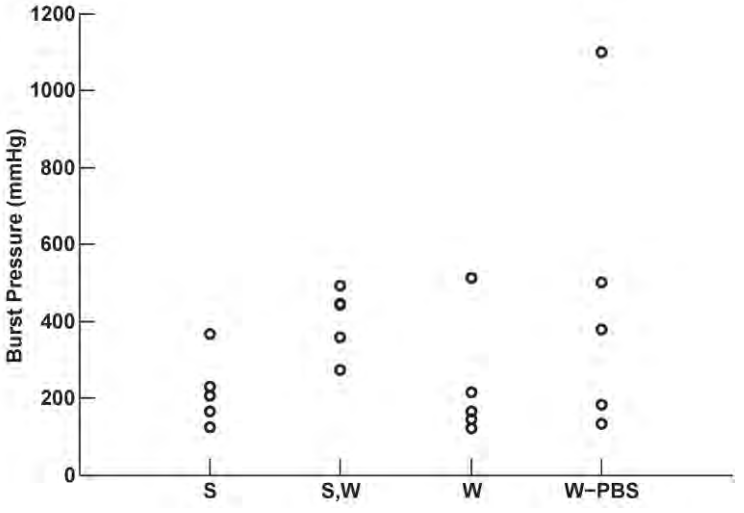

Figure 13: Tensile strength and burst pressure for vessels with sutures only (S), 4 stay sutures and welded albumin (S,W), and vessels welded without sutures (W). After storage in PBS, vessels with stay sutures retained tensile strength and pressure-holding capacity, while vessels without stay sutures lost significant tensile strength. Welds were 3 mm wide and used 2 layers of 38% (w/w) solder denatured at 570 mW.

Task 1-6, In vitro vessel tests

Axial tensile strength testing was performed for all combinations of weld parameters using an 858 Mini Bionix II (MTS Systems, MN) materials tester. Before mounting in the materials tester, 100 mL PBS was passed through the vessel to dissolve the stent. Vessels were anchored on both sides of the weld with aluminum clips and pulled apart at 2 mm/s. The tension was measured with a calibrated gauge (661.11A.02, MTS Systems) and recorded using the software controller for the MTS. The maximum tension for each vessel prior to breaking was recorded.

Tensile strengths increased from 0.6±0.5 to 1.4±0.5 N as the number of layers increased from 1–3 (with W=3 mm, $Csolder$=38%, and P=430 mW) (Fig. 15). Procedure time also increased linearly from 5 to 9 minutes.

Vessels with 1–7 mm wide welds (2 layers of 38% HSA, 430 mW laser power) had average ultimate tensile strengths of 0.6±0.1 N to 0.7±0.3 N (Fig. 15), with 3 mm vessels performing best. Average burst pressures were 13±23 to 150±45 mmHg (Fig. 12), with 3–5 mm welds performing comparably and better than other widths. Three vessels with 1 mm welds, and 2 vessels with 7 mm welds developed holes or separated completely while mounting on the tube fittings for burst testing. No vessels with 3 or 5 mm welds failed in such a premature fashion. Irradiation time increased linearly from 7 to 17 minutes as weld width increased from 1 to 7 mm. Faster anastomoses than those reported here have been achieved in studies currently underway with larger spot sizes and higher powers.

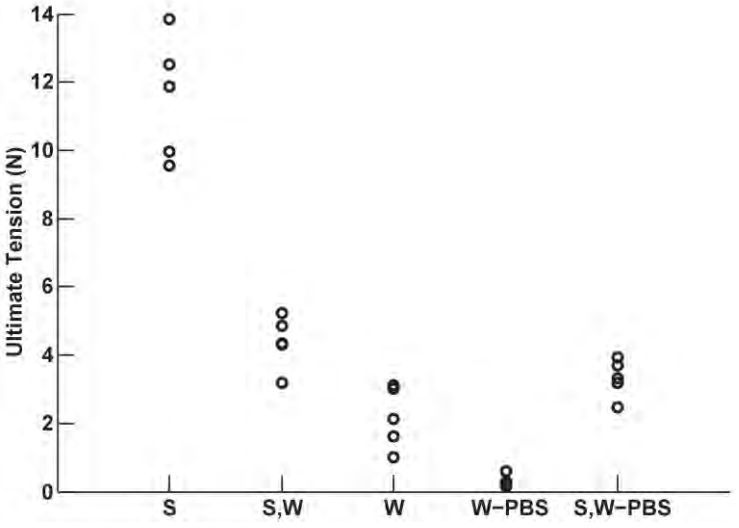

Figure : Tensile strength and burst pressure for vessels with sutures only (S), 4 stay sutures and welded albumin (S,W), and vessels welded without sutures (W). After storage in PBS, vessels with stay sutures retained tensile strength and pressure-holding capacity, while vessels without stay sutures lost significant tensile strength. Welds were 3 mm wide and used 2 layers of 38% (w/w) solder denatured at 570 mW.

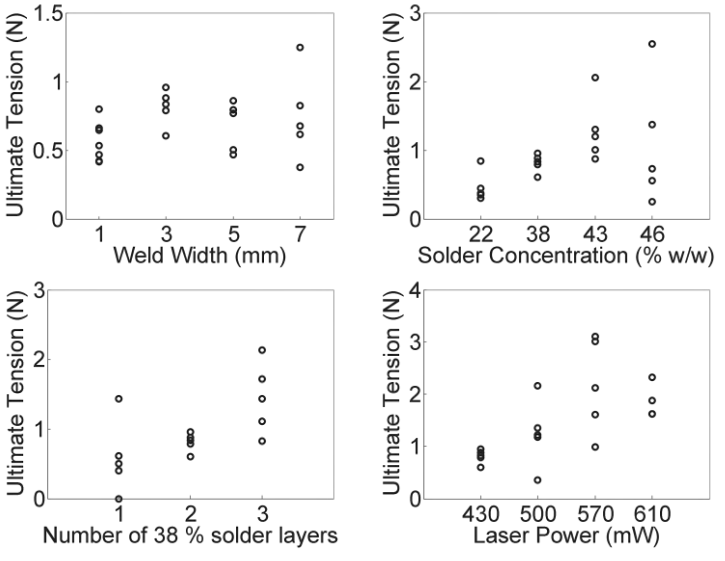

Figure 15: Maximum tension before breaking of (clockwise from upper left) vessels with varied welds widths; varied solder concentrations; varied laser powers; and varied solder layers. N=7 for the W=1 mm weld width test and N=5 for all others.

Task 1-7, Stent packaging

Finished stents were stored individually in 0.5 mL micro centrifuge tubes. Each lot of stents was sealed in an aluminum pouch and γ-irradiated at 25-40 kGy. After sterilization, stents were stored at room temperature in the sterilization packaging.

Task 1-8, Sterility

Stents were sterilized with γ-irradiation, because ethelene oxide sterilization alters them chemically, steam denatures them, and the high viscosity precludes filtration sterilization. It is known that γ-irradiation causes protein fragmentation and aggregation, altering chemical and physical properties. The effect of γ-irradiation on stent solubility was investigated by monitoring stent dissolution without flow.

Task 1-9, In vivo testing

This section describes the surgery outlined in our IACUC application (attached).

Two deviations from the original proposed in vivo testing have been suggested by our surgeons and the IACUC committee. First, that we should use rabbits instead of pigs because rabbits are the lowest species on the phylogenetic tree with appropriately sized arteries for relevant surgical modeling. Second, that the one week study be replaced by an acute study that allows training of the surgeons. The consensus was that the one week time point was too early to ascertain anything about the healing and repair process of the vessel.

Before pursuing a chronic study, a small three animal study will be performed to investigate the method's success at the time of surgery, and to familiarize the surgeons with the new technique and animal model. A 5 cm segment will be removed from each carotid artery, and then replanted. One end of each segment will be anastomosed with conventional sutures following the standard of care, and the other end with the new LAVA method. If the welded vessels remain intact and free of complication after 15 minutes, a chronic study will be conducted to evaluate the vessels long-term ability to stay open and unobstructed (patency). In the chronic study, both carotid arteries in each animal will be resected and then an anastomosis will be performed. One of the carotid arteries will be laser welded with the new LAVA method, and the other sutured following the standard of care. These treatments will be randomized, and the IACUC will be informed of acute study results before progressing with the chronic study. At the end of the 10-week chronic studies, the animals will be humanely euthanized and the welded vessels will be analyzed.

Pre-Operative Care

All experiments will be performed in accordance with the 1996 National Research Council, "Guide for the Care and Use of Laboratory Animal" and applicable Federal regulations.

The rabbits will be socialized to human contact one week prior to surgery with the use of hay and apples to make pre and post-operative handling less stressful. Food and water will be given *ad libitum*. At approximately 30 minutes prior to anesthesia induction, the animals are medicated with Glycopyrrolyte (0.01mg/kg) IM or SQ for blocking vagal stimulation. Animals will be given Enrofloxacin ("Baytril") 5 mg/kg IM at the time of anesthetic induction (one dose) and Ketoprofen 2.5 mg/kg once during surgical preparation to maintain

anesthesia & provide analgesia. Pre-medication will consist of a mixture (same syringe) of Ketamine, 35 mg/kg and Xylazine, 5 mg/kg IM. Rabbits will be sedated with general endotracheal anesthesia using 1-4% isoflurane inhalant administered via endotracheal tube. Intra-operatively, Bupivicaine will be used as a local incisional block and Meloxicam. 0.3 mg/kg SC, will be used as an analgesic. Buprenorphine, 0.01 mg/kg will be given at the time of recovery. An IV catheter is placed into an auricular vein to administer warmed IV fluids (Lactated ringers or Normal Saline given at a rate of 5-10ml/kg/hr) and drugs. After the rabbit is adequately anesthetized, it will be placed in a supine position. The animal neck will be shaved, prepped and draped in a sterile fashion. Strict aseptic technique will be followed during the surgical procedure. During surgery, the animals heart rate, oxygen level, carbon dioxide level and respiration rate will be monitored every 15 minutes.

Laser Anastomosis

During all surgical procedures, strict aseptic technique will be followed. All instruments will be pre-sterilized using an autoclave, and all staff assisting with surgical procedures will follow standard operating procedures for sterile scrub-in and use proper sterile personal protective equipment.

The left or right (randomly assigned prior to surgery) carotid artery will be exposed via midline incision in the neck. Prior to dissection, Verapamil will be given at 0.5 mg/hr intravenous (IV). The carotid will be dissected free from periadventitial tissue. Papaverine solution (120 mg in 60 ml of saline) will be applied locally at site of incision to dilate the artery. Heparin (5,000 u, IV) will be given before clamping the vessels and to be repeated every 90 minutes until the procedure is completed.

The laser that will be used is a Class IV laser emitting light in the infrared. The emission wavelength (1.9 microns) is strongly absorbed by water and therefore cannot cause retinal injury. Moreover, the hazard zone of the device extends only tens of centimeters from the end of the laser hand piece because of the rapid divergence of the beam. Nevertheless, the laser could potentially burn the corneal surface of the eye if used improperly. Consequently, all staff working with this laser will be trained by a laser safety officer and given explicit directives for how to work safely with this particular laser.

In the chronic study, both carotid arteries in each animal will be resected and randomly chosen to receive either the conventional suture anastomosis, or laser-welded anastomosis. In laser-welded anastomoses, an albumin stent matched to the vessel inner diameter

stent will be inserted into both ends of the vessel segment. The anasotomotic edges will be proximated over the stent and secured with four 6-0 Prolene stay sutures at 90-degree intervals. 38-42% albumin solder will be externally applied to the anastomotic site. Laser welding will start with slow rotation from anterior to posterior of the vessel. After completion of laser anastomoses, as determined by uniform light brown color change in the albumin solder, the vascular clamps at proximal and distal end will be released to re-establish the blood flow. If bleeding is observed, clamps will be reapplied for additional spot welding. The entire surgical process is expected to last a maximum of 30 minutes immediately following exposure of the carotid artery. After the procedure is complete, the wound will be closed in a two-layer fashion with 3-0 Vicryl suture.

Postoperative Care and Observation

After surgery, the animals will be returned to their cages in the animal housing area and closely monitored until awake. Animals will be observed for signs of abscess, fever, respiratory failure, and loss of appetite. The key to effective assessment of pain and efficacy of analgesic therapy is knowledge of species-specific, and optimally, animal-specific changes in appearance and behavior post-procedurally. The rabbits will be monitored for post-operative pain by assessing the clinical signs of post-procedural pain. If any of the study animals show these signs, pain-relieving drugs will be administered based on the discretion of the head veterinarian.

Endpoints

The rabbits will be monitored for post-operative pain following the signs listed in 8.3. In addition the rabbits will be observed for (but not limited to) activity level, malaise, appetite, and fatigue. If it appears that the animals are having signs/symptoms of pain and/or distress not relieved with pain medications, they will be anesthetized with a mixture (same syringe) of Ketamine, 35 mg/kg and Xylazine, 5 mg/kg IM and then euthanized via an overdose of barbiturates (Euthanasia solution, 390mg/ml at a dose of 1 ml/5 kg body weight). A bilateral pnemothorax will be created following euthanasia, and the carotid arteries removed for analysis.

Final time point

Prior to euthanasia, animals will anesthetized with a mixture (same syringe) of Ketamine, 35 mg/kg and Xylazine, 5 mg/kg IM. At the final timepoint (60 and 90 days), rabbits will be euthanized via an overdose of barbiturates (Euthanasia solution, 390mg/ml at a dose of 1 ml/5 kg body weight) administered IV while under anesthesia. A bilateral pnemothorax will be created following euthanasia. The anastomosed

carotid artery will be removed and fixed in formalin, then embedded in paraffin, sectioned, and stained with hematoxylin and eosin for histological examination.

Task 1-10, Histology

Stained tissue will be analyzed under magnification for stenosis, hyperplasia, intimal cell growth, pseudoaneurysm and any abnormalities. The degree of stenosis will be quantified by the quotient of the anastomotic luminal diameter and the lumen diameter proximal to the anastomosis. Degree of stenosis will be compared statistically for sutured and laser welded anastomoses.